ARL

US Army Research Laboratory

Modeling Quantum Teleportation with Quantum Tools in Python (QuTiP)

by MG Hager, BT Kirby, and M Brodsky

NOTICES

Disclaimers

US Army Research Laboratory

Modeling Quantum Teleportation with Quantum Tools in Python (QuTiP)

by BT Kirby and M Brodsky
Computational and Information Sciences Directorate, ARL

MG Hager
Cornell University, Ithaca, NY

REPORT DOCUMENTATION PAGE			*Form Approved* *OMB No. 0704-0188*

Public reporting burden for this collection of information is estimated to average 1 hour per response, including the time for reviewing instructions, searching existing data sources, gathering and maintaining the data needed, and completing and reviewing the collection information. Send comments regarding this burden estimate or any other aspect of this collection of information, including suggestions for reducing the burden, to Department of Defense, Washington Headquarters Services, Directorate for Information Operations and Reports (0704-0188), 1215 Jefferson Davis Highway, Suite 1204, Arlington, VA 22202-4302. Respondents should be aware that notwithstanding any other provision of law, no person shall be subject to any penalty for failing to comply with a collection of information if it does not display a currently valid OMB control number.
PLEASE DO NOT RETURN YOUR FORM TO THE ABOVE ADDRESS.

1. REPORT DATE *(DD-MM-YYYY)*	2. REPORT TYPE	3. DATES COVERED (From - To)
December 2017	Technical Report	June 1, 2017–July 31, 2017

4. TITLE AND SUBTITLE	5a. CONTRACT NUMBER
Modeling Quantum Teleportation with Quantum Tools in Python (QuTiP)	
	5b. GRANT NUMBER
	5c. PROGRAM ELEMENT NUMBER
6. AUTHOR(S)	5d. PROJECT NUMBER
MG Hager, BT Kirby, and M Brodsky	
	5e. TASK NUMBER
	5f. WORK UNIT NUMBER

7. PERFORMING ORGANIZATION NAME(S) AND ADDRESS(ES)	8. PERFORMING ORGANIZATION REPORT NUMBER
US Army Research Laboratory ATTN: RDRL-CIN-T 2800 Powder Mill Road Adelphi, MD 20783-1138	ARL-TR-8260

9. SPONSORING/MONITORING AGENCY NAME(S) AND ADDRESS(ES)	10. SPONSOR/MONITOR'S ACRONYM(S)
	11. SPONSOR/MONITOR'S REPORT NUMBER(S)

12. DISTRIBUTION/AVAILABILITY STATEMENT

Approved for public release; distribution is unlimited.

13. SUPPLEMENTARY NOTES

14. ABSTRACT

The unique properties, notations, and conventions of quantum mechanics can make it challenging to properly simulate using traditional software packages. For this reason, several specialized software packages designed for this purpose have recently been released. In this technical report we evaluate one in particular, the Quantum Tools in Python (QuTiP) package, to determine its suitability for use in the simulation of quantum networking protocols. We approach this problem by using QuTiP to implement quantum teleportation, a basic quantum networking operation. We found that QuTiP is technically sound in that it is able to reproduce several published findings, and that it saves significant program design time due to its large library of preprogrammed functions. The only inconvenience we found was that it is only capable of numerical simulation. For these reasons we conclude that QuTiP is a powerful and useful tool for quick tests, and potentially even large numerical simulations.

15. SUBJECT TERMS

quantum teleportation, quantum information, quantum networking, quantum physics, quantum communication, Bell inequality, Bell nonlocality, computational physics, QuTiP

16. SECURITY CLASSIFICATION OF:			17. LIMITATION OF ABSTRACT	18. NUMBER OF PAGES	19a. NAME OF RESPONSIBLE PERSON
			UU	26	Brian Kirby
a. REPORT	b. ABSTRACT	c. THIS PAGE			19b. TELEPHONE NUMBER (Include area code)
Unclassified	Unclassified	Unclassified			391-394-4664

Standard Form 298 (Rev. 8/98)
Prescribed by ANSI Std. Z39.18

Contents

List of Figures

List of Tables

Acknowledgments

INTENTIONALLY LEFT BLANK.

1. Introduction

Quantum mechanics and applications that rely on quantum principles to operate, such as quantum computing, quantum networking, and quantum cryptography, can be difficult to analyze computationally using commonly available software packages. One reason for this is the lack of native functions that are relevant to quantum problems. A second is that notational conventions in physics and computer science differ and can cause confusion. To facilitate the use of computers for the analysis of quantum operations, several software packages created solely for this purpose have recently been released. Some examples include Quantum Tools in Python (QuTiP) (Nation and Johansson 2017), Quantum Entanglement Theory Laboratory (QETLAB) (Johnston 2016), and Forest (Dekant 2017).

In this technical report we will evaluate the utility of QuTiP for the simulation of quantum networking operations by digitally modeling quantum teleportation (Bennett et al. 1993). We will then use this model to reproduce published results related to quantum teleportation when imperfect resource states are used, as well as graph-related metrics, such as fidelity, average fidelity, concurrence, and purity. Specifically, we numerically model the situation where the shared resource is a 2-qubit isotropic state. This scenario is especially interesting because isotropic states can be separable, entangled, or nonlocal, and each of these regimes has published results that can be verified. We further use our program to study the teleportation of mixed input states, which is closely related to entanglement swapping.

This report is organized as follows. In Section 2 we review the quantum teleportation protocol as well as several related results. In Section 3 we describe some specific aspects of QuTiP, and how teleportation was implemented within it. We then use our teleportation program to teleport pure states in Section 4 and mixed states in Section 5.

2. Quantum Teleportation

Quantum teleportation has been a widely researched topic due to its applications in quantum information processing. Despite the colloquial definition, the word teleportation in this context means that the quantum state of one particle is being transferred to another particle, and not the transfer of the particle itself. As initially proposed by Bennett et al. (1993), the only resources required for the transfer of the quantum state from one party ("Alice") to another ("Bob") is a pre-shared Bell state between the 2 parties and a classical channel over which Alice can send 2 bits of classical information to Bob. An illustration of this protocol is provided in Fig. 1.

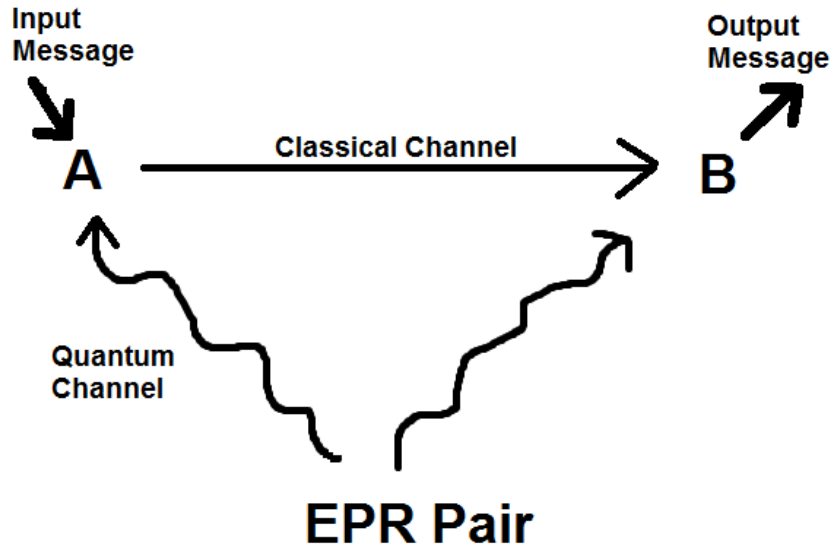Interestingly, this protocol still functions when both users are unaware of what state is being teleported.

Fig. 1   **Diagram of the teleportation protocol**

As 2 classical bits are insufficient to determine the state of a qubit, it is clear that the shared Bell state plays an important role in the transfer of information. One way to investigate this is to determine how successful teleportation is when imperfectly entangled and mixed states are used as the shared resource instead of a Bell state. To compare these situations, a measure called fidelity is used (Popescu 1994), which is defined as follows: If Alice wishes to teleport state $|\chi\rangle$ and, after teleportation, Bob is left with a possibly mixed state ρ_B, then the fidelity of the teleportation is defined as $F = \langle\chi|\rho_B|\chi\rangle$. Since this expression will generally depend on the initial state $|\chi\rangle$, we define the average fidelity $\overline{F}$, which is F averaged uniformly over all possible pure input states.

Recently, much work has been devoted to determining the bounds on the average fidelity for different resource states. The original quantum teleportation protocol has $\overline{F} = 1$, which means that the correspondence between the initial state to be teleported and the state remaining at the end of the protocol is perfect (Popescu 1994). However, if Alice and Bob cannot communicate at all, the best Bob can do is guess, which will result in an average fidelity between Alice's and Bob's states of 1/2 (Popescu 1994). Next, we ask what the average fidelity is if Alice and Bob are restricted to only the classical channel. This corresponds to the original teleportation protocol, but without the shared entangled resource state. In this case, the average fidelity achievable is $\overline{F} = 2/3$ and can be attained by having Alice measuring the state to be teleported along an arbitrary direction (but agreed upon with Bob) and Bob preparing a state in the corresponding direction

(Popescu 1994). From this, any shared resource state between Alice and Bob that results in an average fidelity of $\overline{F} > 2/3$ is considered to be "useful for teleportation" (Horodecki et al. 1996). It has been shown that any state that violates Bell's inequality is a useful resource state for teleportation (Horodecki et al. 1996). Interestingly, the opposite is not necessarily true. Just because a state is useful for teleportation does not mean that it is nonclassical (Popescu 1994). In other words, states have been found which admit a local description, but still result in average teleportation fidelity above 2/3 (Popescu 1994, Gisin 1996, Barrett 2001). Many of these results will be reproduced using isotropic states in the following sections.

We now discuss the teleportation scheme in more detail. Our presentation closely follows that of Rieffel and Polak (2011), but was originally introduced by Bennett et al. (1993). As mentioned above, the goal of quantum teleportation is to transfer a quantum state from one user (called Alice) to another (called Bob) using only a classical channel and a shared entangled resource state. In the original protocol, the shared resource state is a fully entangled Bell pair, which we will write as

$$|\phi^+\rangle = \frac{1}{\sqrt{2}}(|00\rangle + |11\rangle), \tag{1}$$

where $|0\rangle$ and $|1\rangle$ form an orthonormal basis. In this same basis, we can express a general state to be teleported as

$$|\chi\rangle = a|0\rangle + b|1\rangle, \tag{2}$$

with a and b complex numbers that satisfy $|a|^2 + |b|^2 = 1$. Together, the initial state of the entire system can then be expressed as

$$|\chi\rangle \otimes |\phi^+\rangle = \frac{1}{\sqrt{2}}(a|000\rangle + a|011\rangle + b|100\rangle + b|111\rangle), \tag{3}$$

where the notation has Alice's 2 initial qubits first and Bob's last in each bracket. The protocol then begins with Alice performing a Bell state measurement on her 2 qubits and recording the result. A Bell state measurement is an entangling operation that projects the state of 2 qubits onto 1 of the 4 Bell states. In terms of basic quantum gates, this can be achieved using a controlled NOT gate (CNOT gate) followed by a Hadamard transformation and measurements in the standard basis. The Hadamard transformation is a single qubit operation that can be written as

$$H = \frac{1}{\sqrt{2}}(|0\rangle\langle 0| + |1\rangle\langle 0| + |0\rangle\langle 1| - |1\rangle\langle 1|), \tag{4}$$

which operationally takes a single qubit to a superposition. A CNOT gate is a 2-qubit gate and can be written as

$$CNOT = |00\rangle\langle00| + |01\rangle\langle01| + |11\rangle\langle10| + |10\rangle\langle11| . \qquad (5)$$

We see that this operator flips the state of a second qubit if the first qubit is in state 1. The application of these 2 gates to Alice's qubits can be written as

$$(H \otimes I \otimes I)(CNOT \otimes I)(|\chi\rangle \otimes |\phi^+\rangle) = \frac{1}{2}\big(|00\rangle(a|0\rangle + b|1\rangle) + |01\rangle(a|1\rangle + b|0\rangle) + |10\rangle(a|0\rangle - b|1\rangle) + |11\rangle(a|1\rangle - b|0\rangle)\big) , \qquad (6)$$

where I is the identity. We can see from this that a projection of Alice's 2 qubits onto the standard basis will project Bob's state onto one of the four 2-qubit states shown in the first column of Table 1.

Table 1   Bob's output states and the corresponding corrective local unitary operations

ρ_B	Corrective operation
$a|0\rangle + b|1\rangle$	I
$a|1\rangle + b|0\rangle$	σ_X
$a|0\rangle - b|1\rangle$	σ_Z
$a|1\rangle - b|0\rangle$	$i\sigma_Y$

The second column of Table 1 lists what single qubit gate, if applied to Bob's state, would transform it into $|\chi\rangle$. By performing this measurement Alice knows which of these 4 states is in Bob's possession and uses the classical channel to send 2 bits of information to Bob letting him know which corrective operation he should apply to recover $|\chi\rangle$. It is noteworthy that Alice's message qubit is now effectively destroyed and thus its reconstruction by Bob does not violate the No Cloning Principle.

As described, the state Bob ends up with will be an exact duplicate of $|\chi\rangle$. However, any number of factors, such as the entanglement of the resource state and the purity of the inputted message, may cause Bob's final "output" qubit to differ to an extent from Alice's original "input." We will numerically investigate these possibilities in later sections.

3. Implementation

In this section we describe how we digitally simulated the quantum teleportation protocol using the QuTiP package for Python, and discuss some of the preprogrammed functions we found most useful. Operationally, our program functions as described in the previous section in the sense that it takes as an input state to be teleported (or generates its own randomly), applies the CNOT and Hadamard gates, performs a measurement, and finally applies the corrective unitary to the final qubit. For simplicity we often set the program to project onto a specific Bell measurement output so that Bob's corrective operation was fixed. This was done to speed up the program and make it easier to check for errors; however, it is also experimentally motivated by the fact that with linear optics the ψ^- projection can be implemented with only a beamsplitter and 2 detectors.

Our teleportation model, as well as QuTiP itself, is built upon the quantum object class Qobj, a data type that includes the fields dimension, shape, and data in matrix representation. This structure is used as the basis of our program and all states and operators are built using this representation. Specific states were created using the following basic elements: the *basis* function, which allows for the creation of Fock states; the *dag* function, which finds the adjoint of a quantum object; and the *tensor* function, which finds the tensor product of 2 input operators.

Since we are mostly interested in teleporting random input states, rather than a specific input state, it was important for us to be able to produce random pure and mixed density matrices. To accomplish this we can use Numpy's *random* to choose vectors either along the surface of the Bloch sphere (for pure states) or throughout the entire sphere (for mixed states). While this method is straightforward, to improve performance we can also use the *rand_dm(n)* function, which creates a random density matrix of n dimensions.

The gate operations are performed using the built-in functions *cnot* and *hadamard-_transform*, which implement the CNOT gate and Hadamard gate, respectively. After these and the projections onto measurement states, the tracing out of the measured qubits is performed using *ptrace*.

All of our numerical tests are performed with isotropic mixed states as the entangled state resource. These states, which are given by

$$p|\phi^+\rangle\langle\phi^+| + \frac{1-p}{4} I_4 \, , \tag{7}$$

where $-1/3 \leq p \leq 1$ and I_4 (Werner 1989; Horodecki and Paweł 1999) form the identity matrix of dimension 4. We note that these states are equivalent for 2 qubits,

up to local rotations, to the more familiar Werner states (Werner 1989). Also, in what follows we will restrict the range of the isotropic state to $0 \leq p \leq 1$, since this captures the interesting regions of the function and allows us to more easily interface with published results. In QuTiP the isotropic state of 2 qubits can be easily created using functions already described. The reason we focus on these states is because they can range from separable, to entangled, to nonlocal, depending on the value of p. To demonstrate the ease at which we can increment the concurrence of these states we have created Fig. 2, which plots the concurrence of the state as a function of p. We note that when $0 \leq p \leq 1/3$, the concurrence of the isotropic state is 0 and the state is not entangled, and when $p > 1/3$, it is entangled with a concurrence given by $C = (3/2)p - 1/2$. The state also violates the Clauser, Horne, Shimony, and Holt (CHSH) equality (a form of the Bell inequality) when $p > 1/\sqrt{2}$. The region between when the state becomes entangled and when it violates the CHSH inequality is less understood. When considering local projective measurements, it was shown by Werner (1989) that a local hidden variable model exists when $p \leq 1/2$, and this bound was subsequently extended to $p \lesssim 0.66$ by Acin (2006). Therefore, there is a region between $1/3 < p \lesssim 0.66$ where the state is entangled but local. These 3 important values, $p = \frac{1}{3}, p \approx 0.66$ and $= 1/\sqrt{2}$, are marked by vertical lines in Fig. 2. For an overview of recent progress on bounding the value of p needed to reveal nonlocality see Brunner (2014).

In order to generate graphs numerically, we use QuTiP's metrics module. We use the *concurrence* function to find the concurrence of the isotropic resource state, and the *fidelity* function to measure the fidelity between the input state and the final state in Bob's possession. We rounded these metrics to 5 decimal places as this sufficiently met our needs and eliminated incongruities due to rounding in earlier computations. We also note that, in order to match the conventional definition, we have to square the output of the *fidelity* function (Nielsen and Chuang 2002).
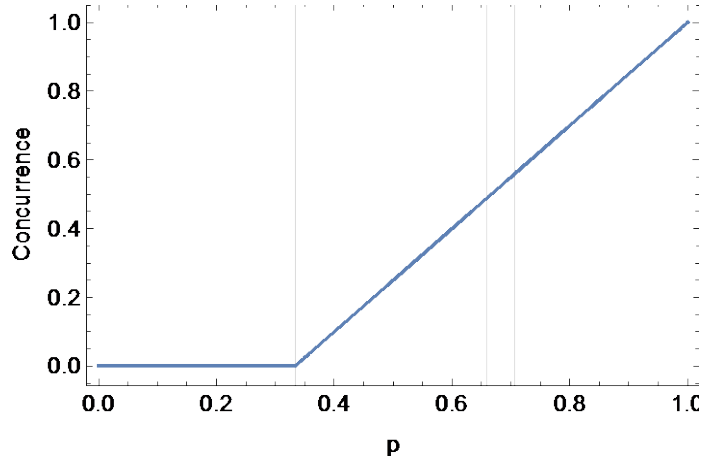
Fig. 2 **Isotropic resource state parameter p vs. the concurrence of the isotropic state. The vertical lines are placed at $p = \frac{1}{3}, p \approx 0.66$ and $p = 1/\sqrt{2}$.**

4. Teleporting Pure States

We begin by investigating the teleportation fidelity as a function of the p parameter of an isotropic resource state by generating multiple instances of the teleportation protocol and creating a point plot. In this special case of a pure input state and an isotropic resource state, the fidelity and average fidelity are equivalent and hence we only need to plot 1 point for each p of the isotropic state (Bandyopadhyay and Sanders 2006). The resulting plot is shown in Fig. 3, and has 1 point for every .01 change in p. For convenient comparison to Fig. 2, we have also included the vertical lines of Fig. 2, which demarcate the regions where the isotropic state is separable, entangled, and nonlocal. Additionally we have included 2 horizontal dashed lines, the green one at a fidelity of 1/2, representing the achievable fidelity if there were no channel between Alice and Bob, and the second red dashed line at a fidelity of 2/3, the maximum achievable when Alice and Bob only share a classical channel. Further explanation for these fidelities is given in Section 2.
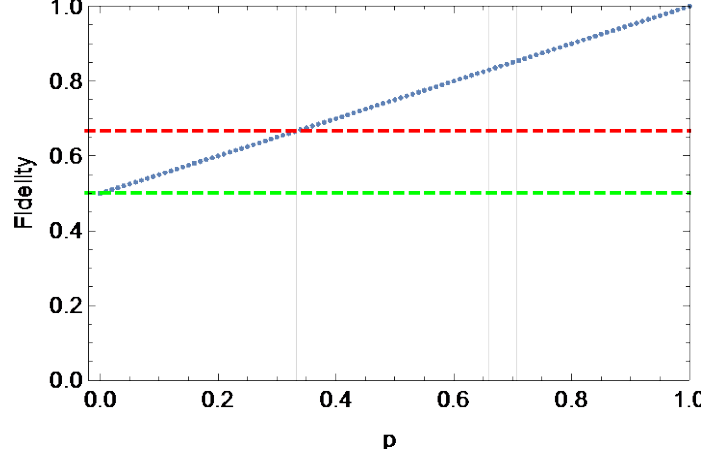
Fig. 3 **Isotropic resource state parameter p vs. the fidelity of a teleported message. The vertical lines are placed at $p = \frac{1}{3}, p \approx 0.66$ and $p = 1/\sqrt{2}$. The horizontal lines are given by $F = \frac{1}{2}$ and $F = \frac{2}{3}$.**

The values we see in Fig. 3 are in line with our expectations. While the isotropic state is separable ($p \leq 1/3$), the fidelity is bounded by 2/3, which is the maximum possible with only a classical channel. More generally, this plot fits the predictions of Bandyopadhyay and Sanders (2006), which derived for the expression

$$F = \frac{1}{2} + \frac{p}{2} \tag{8}$$

for the teleportation fidelity when an isotropic state is used as the resource. An intriguing aspect of this plot and the expression above is that we see there are regions where the isotropic state is useful for teleportation $\left(F > \frac{2}{3}\right)$, but that the isotropic state itself admits a local model ($p \lesssim 0.66$). It is precisely this observation that indicates that nonlocality and usefulness for teleportation are not equivalent. We see that it is in fact entanglement which is necessary for teleportation fidelities greater than 2/3, but not necessarily nonlocality.

To emphasize the importance of entanglement, but not necessarily nonlocality, to teleportation, we have also created Fig. 4. Here, we plot the teleportation fidelity as a function of the concurrence of the isotropic resource state. For emphasis, we have added the same green and red dashed lines as in Fig. 3. It is important to note that when the concurrence (C) is greater than zero, the isotropic resource state is entangled but not necessarily nonlocal. This fits with the conclusion found from Fig. 4 that entanglement is the essential ingredient for teleportation to be useful and not nonlocality.

We will now connect Fig. 4 to results found in the literature. A direct application of the analysis found in Roa et al. (2016) to the isotropic state we are considering

here results in the following expression for the fidelity of a transported state when the concurrence (C) of the isotropic state is greater than zero ($p > 1/3$):

$$F = \frac{2}{3} + \frac{C}{3}.$$
(9)

This matches up to the regions of Fig. 4, where $0 < C \leq 1$. Additionally, it can be shown directly from the analysis by Roa et al. that for the region where C=0 ($0 \leq p \leq 1/3$), the fidelity is given by

$$F' = \frac{2}{3} + \frac{C'}{3},$$
(10)

where $C' = (3p - 1)/3$. We note that when $p > 1/3$, $C = C'$.
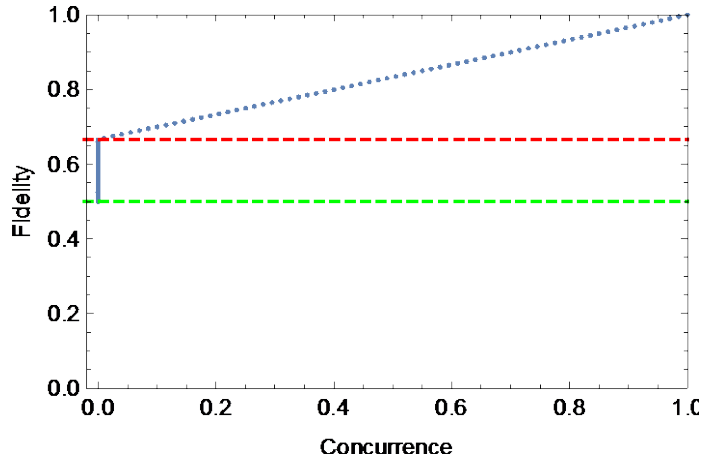

Fig. 4   Concurrence of an isotropic resource state vs. the fidelity of a teleported message. The horizontal lines are given by $F = \frac{1}{2}$ and $F = \frac{2}{3}$.

5.   Teleporting Mixed States

More realistically, the state to be teleported will not be pure but mixed; we also modeled this scenario. This requires a more general definition of teleportation fidelity than the one introduced in Section 2, because now both states can be mixed, instead of just the output state as assumed in the original definition. Here we use the analogous definition where fidelity is calculated between 2 different density matrices ρ and σ using

$$F' = Tr\left[\sqrt{\sqrt{\rho}\sigma\sqrt{\rho}}\right]$$
(11)

rather than between a density matrix and a pure state (Nielsen and Chuang 2002). The average fidelity is now averaged over all mixed input states as well as pure

input states. As with the previous section, we assume here that the shared resource state is an isotropic state.

To begin with, we have produced Fig. 5 by plotting the output fidelity of the teleportation versus the concurrence of the isotropic resource state. The mixed input states are randomly generated by a QuTiP function as described in Section 3. For each of the 100 horizontal values of concurrence we have run the teleportation protocol 50 independent times and plotted each point. It is clear to see that the possible range of fidelities is bounded below by those of a pure state and above by F=1. In Fig. 6 we have generated a similar plot by averaging the values for each concurrence rather than drawing all points. Again, it is clear that the fidelity is higher on average than that which we saw when plotting for pure states. This can be interpreted as saying that the fidelity of a pure state input and its mixed state output is smaller than the fidelity of a mixed state input and its corresponding mixed state output.
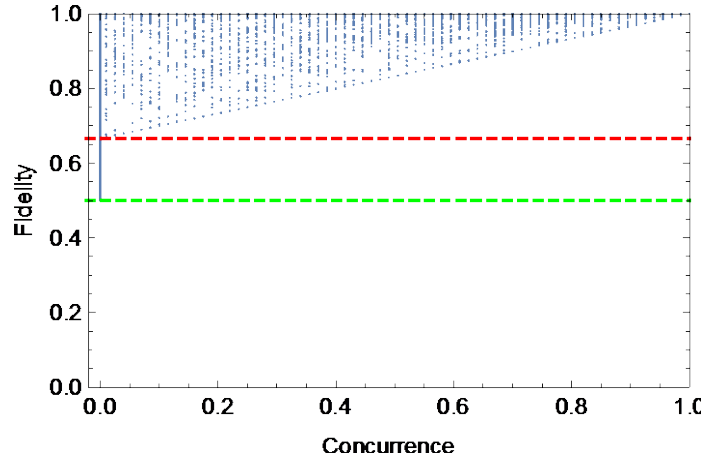

Fig. 5 **Output fidelity vs. concurrence of isotropic resource state. Input states are randomly generated mixed states. The horizontal lines are given by $F = \frac{1}{2}$ and $F = \frac{2}{3}$.**

Fig. 6 **Average output fidelity vs. concurrence of isotropic resource state. Input states are randomly generated mixed states. The horizontal lines are given by $F = \frac{1}{2}$ and $F = \frac{2}{3}$.**
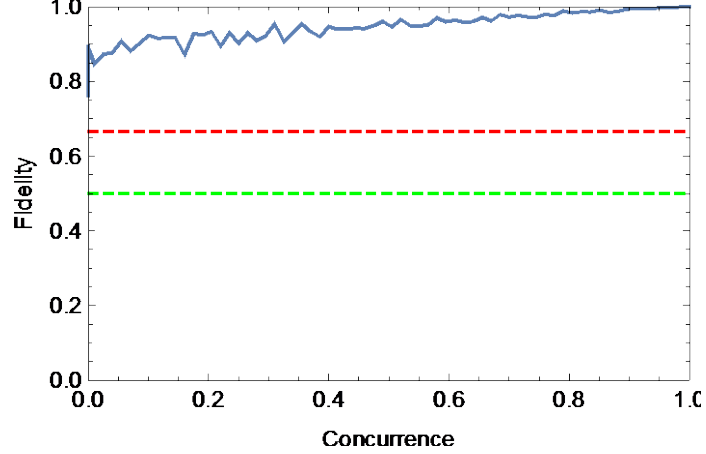
To investigate this phenomenon in a more controlled fashion we define a single qubit state, which is parameterized as follows

$$\rho_q = q(|\omega\rangle\langle\omega|) + (1 - q)(I_2) , \tag{12}$$

where I_2 is the identity matrix of dimension 2 and

$$|\omega\rangle = \frac{1}{\sqrt{2}}(|0\rangle + |1\rangle) . \tag{13}$$

We see that when q=1, the state is a totally pure superposition of the basis vectors and when q=0, it is in a totally mixed state. Using this state, we have created Fig. 7, which plots the teleportation fidelity as a function of the isotropic states p parameter for 100 horizontal values of p and 10 different values of q.

We conclude from this short investigation into the teleportation of mixed states that, since it would generally be expected that the quality of teleportation will decline as the purity of the input state decreases, fidelity may not be the appropriate metric to study this scenario. This notion merits further investigation.
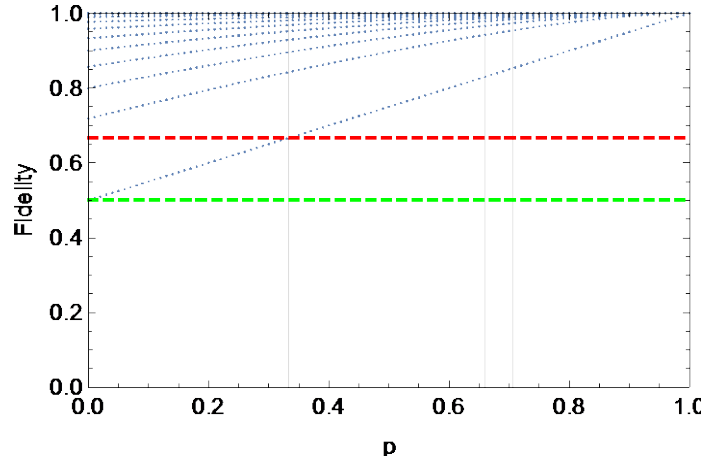
Fig. 7   **Fidelity vs. p parameter of isotropic resource states for mixed input states ρ_q. The vertical lines are placed at $p = \frac{1}{3}, p \approx 0.66$ and $p = 1/\sqrt{2}$. The horizontal lines are given by $F = \frac{1}{2}$ and $F = \frac{2}{3}$.**

6.   Conclusion and Discussion

Modern technologies such as QuTiP make it possible to model fundamental aspects of quantum mechanics, including quantum teleportation. The conclusions derived can widely span fields including quantum networking, quantum information, and quantum computing, and can directly influence experimental work, such as the ongoing construction of our quantum networking test-bed at the US Army Research Laboratory (ARL), pictured in Fig. 8. With a simple Python program built using the Quantum Tools in Python package, we were able to reproduce several published theoretical results. Thus, QuTiP proved useful and reliable for modeling quantum phenomena. We also found QuTiP to significantly reduce the time required to design and implement quantum protocols due to the large number of preprogrammed functions and the fact that the notation used in these functions is that of quantum mechanics. We chose QuTiP for our modeling because it is one of the largest and best maintained quantum software packages; however, it is not necessarily optimized for the application we chose, since its main purpose is the modeling of open quantum systems. We note this because, although it is not advertised to have this feature, we found the lack of an analytical solver to be inconvenient. The authors think that QuTiP is a useful tool and hope that such techniques as described here will continue to be used to advance our knowledge of quantum behaviors.
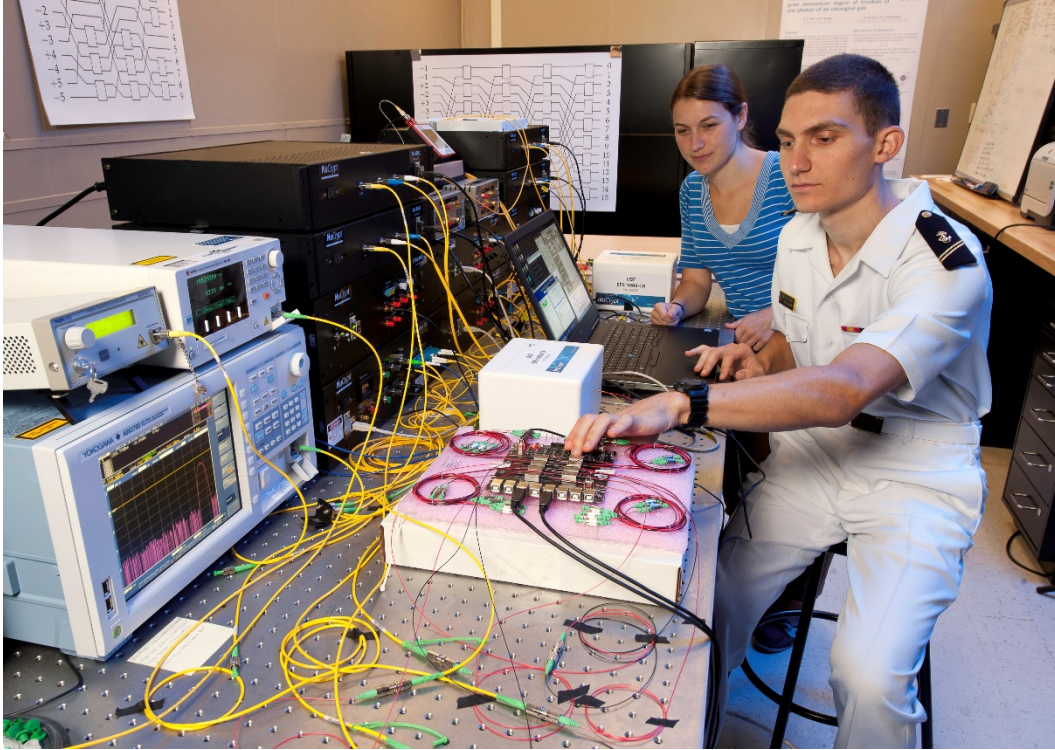
Fig. 8 **Summer intern Mary Grace Hager teams up with midshipman Drew Weninger to learn how to operate the ARL quantum network test-bed**

7. References

Acín A, Gisin N, Toner B. Grothendieck's constant and local models for noisy entangled quantum states. Phys Rev A. 2006;73(6):062105.

Bandyopadhyay S, Sanders BC. Quantum teleportation of composite systems via mixed entangled states. Phys Rev A. 2006;74(3):032310.

Barrett J. Implications of teleportation for nonlocality. Phys Rev A. 2001;64(4):042305.

Bennett CH, Brassard G, Crépeau C, Jozsa R, Peres A, Wootters WK. Teleporting an unknown quantum state via dual classical and Einstein-Podolsky-Rosen channels. Phys Rev Lett. 1993;70(13):1895.

Brunner N, Cavalcanti D, Pironio S, Scarani V, Wehner S. Bell nonlocality. Rev Mod Phys. 2014;86(2):419.

Dekant H, Tregillus H, Tucci R, Yin T. Python tools for reading, writing, compiling, simulating quantum computer circuits. 2017 July 27 [accessed 2017 Nov 9]. https://github.com/artiste-qb-net/qubiter.

Gisin N. Nonlocality criteria for quantum teleportation. Phys Lett A. 1996;210(3):157–159.

Horodecki M, Paweł H. Reduction criterion of separability and limits for a class of distillation protocols. Phys Rev A. 1999;59(6):4206.

Horodecki R, Horodecki M, Horodecki P. Teleportation, Bell's inequalities and inseparability. Phys Lett A. 1996;222(1):21–25.

Johnston N. QETLAB: A MATLAB Toolbox for Quantum Entanglement. 2016 January 12 [accessed 2017 Nov 9]. http://www.qetlab.com.

Nation P, Johansson R. QuTiP: Quantum Toolbox in Python. 2017 July 28 [accessed 2017 Nov 9]. http://qutip.org.

Nielsen MA, Chuang I. Quantum computation and quantum information. Cambridge (UK): Cambridge University Press; 2002.

Popescu S. Bell's inequalities versus teleportation: what is nonlocality? Phys Rev Lett. 1994;72(6):797.

Rieffel EG, Polak WH. Quantum computing: A gentle introduction. Cambridge (MA): MIT Press; 2011.

Roa L, Gómez R, Muñoz A, Rai G, Hecker M. Entanglement thresholds for displaying the quantum nature of teleportation. Ann Phys. 2016;371:228–38.

Werner RF. Quantum states with Einstein-Podolsky-Rosen correlations admitting a hidden-variable model. Phys Rev A. 1989;40(8):4277.

Wiseman HM, Jones SJ, Doherty AC. Steering, entanglement, nonlocality, and the Einstein-Podolsky-Rosen paradox. Phys Rev Lett. 2007;98(14):140402.

INTENTIONALLY LEFT BLANK.

List of Symbols, Abbreviations, and Acronyms

ARL   US Army Research Laboratory

CHSH Clauser, Horne, Shimony, and Holt

CNOT controlled NOT

QETLAB Quantum Entanglement Theory Laboratory

QuTiP Quantum Tools in Python

1 (PDF)	DEFENSE TECHNICAL INFORMATION CTR DTIC OCA

2
(PDF)
	DIR ARL
	IMAL HRA
	  RECORDS MGMT
	RDRL DCL
	  TECH LIB

1 (PDF)	GOVT PRINTG OFC A MALHOTRA

2
(PDF)
	ARL
	RDRL CIN T
	  B KIRBY
	  M BRODSKY